44 p

UNPUBLISHED PRELIMINARY DATA

RADAR INVESTIGATION OF METEORS AT HIGH RATES OF DETECTION

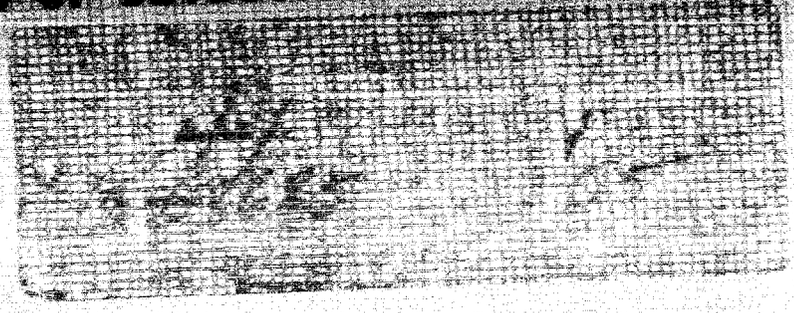

By
C. ELLYETT
C. S. L. KEAY
E. C. McLAUCHLAN

FINAL REPORT.
RESEARCH GRANT No.: NsG - 219 - 62

The research reported in this Document has been Sponsored by

OFFICE OF SPACE SCIENCES
NATIONAL AERONAUTICS AND SPACE ADMINISTRATION
WASHINGTON 25, D.C.

OTS PRICE

$2.00 ph
$0.50 mf

RADIO FIELD STATION
PHYSICS DEPARTMENT
UNIVERSITY OF CANTERBURY
CHRISTCHURCH 1, NEW ZEALAND

SEPTEMBER, 1963

FINAL REPORT - N.A.S.A. RESEARCH GRANT No.: NsG-219-62

In addition to this Final Report, publications supported by the above Research Grant include:

RESEARCH REPORT No.1

"The Distribution of Meteors Around the Earth's Orbit" - C.S.L. Keay.

Monthly Notices of the Royal Astronomical Society, Vol. 126, p.165, 1963.

RESEARCH REPORT No.2

"The Annual Variation in the Radiant Distribution of Sporadic Meteors" - C.S.L. Keay.

Journal of Atmospheric and Terrestrial Physics, Vol. 25, p.507, 1963.

RESEARCH REPORT No.3

"A Practical Method for Determining the Directivity of H.F. and V.H.F. Antenna Systems", - C.S.L. Keay and R.E. Gray.

August 1963.

ABSTRACT

30502

The construction and operation of an improved type of radar system for delineating meteor radiants is discussed. High rates of detection, quite often exceeding 1000 meteors per hour, have been obtained. It is found that the very faint meteors which are detected in such large numbers completely obliterate many of the recognised showers.

Author

1. INTRODUCTION.

The classic method of delineating meteor shower radiants from radar observations is that due to Clegg (1948a, 1948b), which utilises the directive properties of an antenna array in conjunction with the specular reflection of radio waves by a meteor trail. Meteors emanating from a given radiant are generally detected only when the radiant passes through the plane normal to the line joining the observing station and the meteor trail in the antenna beam. When the recorded echoes are plotted as a function of time and range the characteristic range-time envelopes of the Clegg method are obtained. From their shape and time of occurrence the co-ordinates (right ascension, α , and declination, δ) of the radiant may be deduced. If two antennas are used (Aspinall, Clegg and Hawkins, 1951) the accuracy of the radiant coordinates obtained is greatly improved.

When more than 1000 echoes per day have to be plotted the Clegg method becomes too laborious and time-consuming. A modified approach due to Keay (1957) enables the radiant coordinates to be determined by plotting echo rate from both antennas as a function of time. Only those echoes which lie in a range interval straddling the range of maximum occurrence need be used.

This "partial rate method", as it is called, speeds the data processing and allows higher echo rates to be dealt with.

Both methods lead to ambiguities whenever two or more radiants are simultaneously active. These may be resolved, at the price of increased system complexity, by incorporating a third antenna, the beam of which should be spaced equally in azimuth with the other two. Each radiant then produces a time-displaced sequence of peaks in the partial rate curves and it becomes very much easier to relate the individual peaks to one another, or show their non-relationship, as the case may be. If three range intervals are recorded from each of the three antennas nine partial rate curves are obtained, thus giving a nine-fold check on the validity of a radiant. This is discussed in more detail in Chapter 5 and some examples of its application are given in Chapter 6.

The importance of this augmented partial rate method lies in its ability to delineate the radiants of minor showers which produce too few large meteors to make the ordinary Clegg method feasible. Or, putting the matter another way, this method is capable of detecting the presence of shower structure in the sporadic meteor background level.

2. THE TRIPLE-BEAM SYSTEM.

When this work commenced, three narrow beam antenna arrays for operation at a frequency of 69 Mc. were already in existence. Two of them are multiple Yagi arrays directed towards fixed azimuths of 67.5 and 112.5 degrees east of north respectively (Ellyett, Keay, Roth and Bennett, 1961), while the third is a rotatable planar array of half-wave dipoles which can be turned towards any azimuth (Ellyett and Roth, 1955). The Yagi arrays each consist of eight seven-element Yagi antennas giving a beam 4.5 degrees wide in azimuth. For both of them the elevation of the beam is 10 degrees and the power gain approximately 400. The rotatable array comprises twelve half-wave dipoles (3 high by 4 across) mounted one eighth wavelength in front of a reflecting screen. Its main beam is 22 degrees wide in azimuth and directed at an elevation of 12 degrees, giving a power gain of about 80.

In order to provide three beams equally spaced in azimuth the rotatable array is directed to 90 degrees east of north. By using each antenna for transmitting as well as receiving the aerial requirements would have been met had it not been for difficulties encountered in connection with the necessary spark-gap

transmit-receive switching. Unreliability, noisiness and breakthrough all combined to force the abandonment of spark-gaps as a means to this end. In addition it was considered desirable, if possible, to use one transmitter for the whole system instead of having one for each antenna. Accordingly a single wide-beam transmitting antenna was built capable of floodlighting the region searched by the three narrow-beam antennas, which could then be used for reception only. A plan of the actual coverage of the antennas is shown in Figure 1. The shape of the radiation pattern of the transmitting antenna led to it being referred to as a fan-beam antenna: it is fully described in Chapter 3. Although the power gain of the fan-beam antenna is low, this loss has been offset by the elimination of spark-gap switching and has led to better overall system performance.

For the triple-beam system three separate receivers are needed. Two were already in existence and a third was built together with a new display system capable of presenting the three outputs simultaneously for recording on film. These components are described in Chapter 4. A block diagram of the entire system is shown in Figure 2.

The master control unit was also in existence and very little modification was required to make it supply

all of the necessary timing wave forms. Its block diagram is shown in Figure 3. The 150 c/s. repetition frequency for the 69 Mc. transmitted pulses (p.r.f.) was derived from the 50 c/s mains supply frequency, with provision for phase shifting to avoid bursts of interference which are sometimes locked to the supply frequency. The 150 c/s p.r.f. controls the output from a 900 Kc/s crystal oscillator by means of a gating circuit and resets the subsequent pulse divider stages which provide range-markers and other essential timing waveforms following each transmitted pulse. Thus the advantages of crystal control are combined with those of mains-locked operation.

3. THE FAN-BEAM ANTENNA.

This antenna was required to provide, as simply as possible, an azimuthal distribution of radiated power which would enable all three narrow beam arrays to receive meteor echoes. By iterative calculations it was found that a vertical stack of dipoles spaced 0.35 of a wavelength in front of a reflecting screen would produce the required azimuthal pattern. The gain factors used in the design are given in TABLE 1, the notation of which applies to the array geometry shown

α^{o}	$F_{o}(90-\alpha)$	$G^{2}_{\frac{1}{2}},\ 0.7(\alpha)$	Product
0	1.000	1.6181	1.6181
5	0.995	1.6278	1.6197
10	0.978	1.6564	1.6200
15	0.955	1.7015	1.6249
20	0.914	1.7592	1.6079
25	0.868	1.8243	1.5835
30	0.817	1.8896	1.5438
35	0.758	1.9470	1.4758
40	0.696	1.9870	1.3830
45	0.627	1.9999	1.2539
50	0.557	1.9754	1.1003
55	0.490	1.9050	0.9335
60	0.418	1.7820	0.7449
65	0.346	1.6026	0.5545
70	0.275	1.3668	0.3759
75	0.205	1.0779	0.2210
80	0.141	0.7453	0.1051
85	0.080	0.3810	0.0305
90	0.000	0.0000	0.0000

$$G^{2}_{\frac{1}{2}},\ 0.7(\alpha) = \frac{\text{Sin } 2(0.5\pi - 0.7\pi \text{ Cos } \alpha)}{\text{Sin } (0.5\pi - 0.7\pi \text{ Cos } \alpha)}$$

TABLE 1 Gain factors for calculating the horizontal radiation pattern of the Fan-Beam Antenna.

in Figure 4.

The vertical radiation pattern of the fan-beam antenna had to be compatible with those of the three narrow-beam arrays, although it was considered that a slight increase in elevation of the main lobe would be beneficial, for the following reason: Previously, when each of the Yagi arrays were used for both transmitting and reception, the number of received meteor echoes as a function of range peaked near 400 Km, but subsequent work (Keay and Ellyett, 1961) showed that this range should be shortened a little in order to reduce the bias towards detecting radiants passing close to the local zenith. Accordingly, an elevation of 15 degrees was chosen for the main lobe of the fan-beam antenna, leading to an elevation of $12\frac{1}{2}$ degrees for the composite pattern with the Yagi arrays and $13\frac{1}{2}$ degrees for that with the rotatable array. As a result, for each antenna, the peak in the range distribution of meteor echoes is shifted back by about 50 Km, without incurring any appreciable loss in antenna power gain.

The above design requirements were satisfied by using a vertical stack of three half-wave folded dipoles spaced half a wavelength apart, with the lowest dipole one quarter of a wavelength above a ground screen, as indicated in Figure 4. The gain factors used are given

in TABLE 2. Several other designs were considered, but this one has the advantage of a null at 40 degrees elevation which reduces the effect of the principal secondary lobes present in the other arrays near that angle of elevation.

The half-wavelength spacing of the folded dipoles made feed and matching arrangements very simple. Each of the three elements was fed equally in amplitude and phase. The impedance match to the transmission line was very close to optimum, with only a small adjustment of a quarter wave support stub being necessary to bring the standing wave ratio to less than 1.1.

When it was completed the performance of the fan-beam antenna proved to be very satisfactory. Measurements of its directivity were made using a balloon technique (Keay and Gray, 1963) yielding the results shown in Figures 5 and 6. Figure 7 is a photo of the antenna.

The horizontal radiation pattern has a slight dip at azimuth 90 degrees east which indicates that the radiating elements are a little too far away from the reflecting screen. The difference in pattern is so slight that no correction has been made.

The vertical radiation pattern is also fairly close to the calculated design. The main lobe appears to be

β^{o}	$F^{3,\ 0.5(90-\beta)}$	$G_{\frac{1}{2}}^{2,\ 0.7(\beta)}$	$G_{\frac{1}{2}}^{2,\ 1.5(90-\beta)}$	Product
0	3.000	1.618	0.000	0.000
5	2.926	1.628	0.799	3.806
10	2.710	1.656	1.460	6.552
15	2.375	1.702	1.878	7.591
20	1.952	1.759	1.999	6.864
25	1.481	1.824	1.826	4.933
30	1.000	1.890	1.414	2.672
35	0.539	1.947	0.852	0.894
40	+0.128	1.987	+0.223	0.057
45	-0.213	2.000	-0.382	0.163
50	-0.486	1.975	-0.908	0.872
55	-0.684	1.905	-1.317	1.716
60	-0.827	1.782	-1.614	2.379
65	-0.916	1.603	-1.808	2.655
70	-0.957	1.367	-1.919	2.510
75	-0.989	1.078	-1.974	2.105
80	-0.998	0.745	-1.995	1.483
85	-1.000	0.381	-2.000	0.762
90	-1.000	0.000	-2.000	0.000

TABLE 2 Gain factors for calculating the vertical radiation pattern of the Fan-Beam Antenna.

one degree lower than anticipated, but this may be due to errors of measurement. The upper lobe is much broader than the calculated size, due to the limited height of the reflector screen, which was restricted by the need to have clearance between it and a 200 Mc. rotatable array mounted on the same structure (see Figure 7). The resulting backward radiation from the uppermost dipole completely accounts for the broadness of the upper lobe.

4. RECEIVERS AND DISPLAY.

The detection system may be divided into three main components:

1. Three identical receivers
2. Video pulse delays and mixing unit
3. Display and camera

4.1 THE RECEIVERS.

Following the experience gained during meteor rate surveys (Ellyett and Keay, 1963) two additional receivers were constructed, some modifications being incorporated. A block diagram of these receivers is shown in Figure 8, and a photo of one of them in Figure 9. To satisfy the requirement for a sensitive

low noise receiver, a two stage R.F. amplifier is used. The first stage is an ECC88 (6DJ8) neutralised cascode, inductively coupled to the antenna; while the second stage is a conventional pentode amplifier (6AK5). The oscillator and mixer are also conventional. The mixer anodes are tuned to 11.4 and 11.8 Mc. respectively to provide outputs to the two I.F. units via separate 6AK5 pre-amplifiers. A negative suppression pulse from the master control unit is applied to these preamplifiers during transmitter firing.

The main signal I.F. unit of 60 Kc. bandwidth centred on 11.4 Mc. comprises four stages of synchronously tuned amplification prior to the 6AL5 signal detector. Negative-going pulses derived from the sub I.F. unit during the incidence of man-made interference of a transient nature are applied to the last two tuned stages, reducing considerably the effects of pulse type interference.

The sub I.F. unit of 300 Kc. bandwidth is centred on 11.8 Mc. Four stages of synchronously tuned amplification are again used. The output of this unit will be noise only as the centre frequency is 400 Kc. above the signal I.F. frequency. Also, since a shorter time delay is experienced in this wide-band amplifier,

noise pulses due to switching transients, etc. will appear at the output before reaching the signal detector. A pulse shaping and limiting stage after the noise detector is so adjusted that all noise pulses of greater amplitude than the normal background white noise will be applied as negative going suppression pulses to the control grids of the last two tuned stages of the signal I.F. unit via a short time-constant circuit, suppressing the noise pulses coming through the main I.F. unit.

The video compression amplifier has already been fully described (McLauchlan, 1960). However, for completeness a brief description follows: Essentially, the resistive load of a CV138 compression amplifier is shunted by a CV138 cathode follower whose bias is made a function of the integrated white noise. This bias voltage is the rectified output of a CV138 control amplifier, the rise time of which is such that it does not respond to short pulse signals. Further integration of the white noise component of the received signal is achieved by using a relatively long time-constant network in the rectifier output.

4.2 VIDEO PULSE DELAYS AND MIXING UNIT.

The video delays and mixing unit (Fraser, 1961) allow the simultaneous display of the outputs of all three receivers on a single cathode-ray tube display unit, as indicated by the block diagram in Figure 10. The circuit is shown in Figure 11.

Meteor echoes received by Receiver-1 will appear on the intensity modulated cathode-ray tube as double dots, alternate sweeps of the time base being shifted along the range axis by a 75 c/s square wave from the master timer. The dot spacing is adjusted to be equivalent to a time interval of 50 microseconds. Alternate meteor-echo pulses received by Receiver-2 are delayed 50 microseconds by the associated delay line and video gating circuit. Meteor echoes received by this receiver will thus appear on the display tube screen as double dots displaced 100 microseconds along the range axis. Correspondingly, alternate echo pulses received by Receiver-3 will be displaced 150 microseconds along the range axis by a similar process using a 100 microsecond delay line.

4.3 DISPLAY AND CAMERA

The display unit follows conventional practice. An intensity modulated Philips DB 10/78 cathode-ray tube presentation is photographed on continuously moving Ilford 5G91 35mm film. The camera uses 24 feet of film per day.

5. THEORY AND CALCULATIONS

The basic theory underlying the partial-rate method has already been published (Keay, 1957) and needs no modification when three instead of two narrow-beam antenna are employed. The counting of meteors in more than one range-band has also been described in a paper (Ellyett, Keay, Roth and Bennett, 1961) in which it is referred to as a multiple rate-count method, and an example of its usefulness was given. It is the combination of these methods which is referred to as the augmented partial-rate method.

Briefly, short time-interval counts of meteor echoes, whose ranges lie in a band centred on the range of maximum occurrence, give a partial-rate curve when plotted against time. The times when peaks occur in the partial rate curves from two or more antennas yield

the radiant coordinates of the meteor activity which gave rise to the peaks. The same is true when meteors in range-bands adjacent to the central range-band are used, although care must be taken to allow for the assymmetrical distribution of meteors within the range-band when high accuracy is required.

The manner in which the radiant coordinates result from the observed times of occurrence of peaks in meteor rate may be seen from Figure 12. This Figure represents a horizontal projection of the intersection with the celestial hemisphere of the planes in which meteor trails must lie in order to be detectable at the range concerned. It is the same as saying that meteors from a given radiant are only detectable as the radiant passes through the appropriate "collecting" plane. For the easterly directed antenna the collecting planes for echoes detected near ranges of 300,400 and 500 Km intersect the celestial hemisphere in the lines N1S, N2S and N3S respectively. In reality the lines are narrow strips due to the finite size of the range interval in which echoes are counted (each "range-band" extended 50 Km on either side of the nominal range, i.e. the range intervals were 100 Km wide) and to the spread in azimuth of the antenna beam.

As a specific example, the radiant 'A' will first produce echoes in the 500 Km range-band of the South of East antenna (at point 'a' in Figure 11), then in its 400 Km range-band at a time which happens to coincide with the meridian passage of the radiant in this particular case (point 'b'). Echoes will next appear in the 500 Km range-band of the East antenna (point 'c') and almost at the same time in the 300 Km range-band of the South of East antenna (point 'd'). And so on. The important point is that the order of appearance of echoes in the range-bands of the three antennas will be quite different for radiant 'B', and is a function of the radiant declination. However, up to quite high values of declination, the order of appearance of echoes in the various range bands associated with a <u>given</u> antenna is always the same. Also, except for radiants passing within a few degrees of the zenith, the peak echo rate in a given range-band from the East antenna is always mid-way in time between the peak rates in the same range-band from the other two antennas. These characteristics enable discrete meteor shower activity to be identified whenever it occurs.

For each range-band of the three antennas the time differences between peak echo rate and the time of meridian passage (local transit) of any culminating

TABLE OF AERIAL COLLECTING PLANE TRANSIT TIMES

COMPUTED FOR LATITUDE -43.62 DEGREES

AERIAL AZIMUTH (EAST) = 112.5 DEGREES

ECHO HEIGHT = 95.0 KILOMETERS

SLANT RANGE OF MEAN ECHO = 500.0 KILOMETERS

ELEVATION OF MEAN ECHO = 8.75 DEGREES

MAXIMUM DECLINATION = 67.74 DEGREES

DECLINATION VALUE AT HORIZON = 41.97 DEGREES

DECL.	HOUR ANGLE	DECL.	HOUR ANGLE	DECL.	HOUR ANGLE
		19	-0 H 5.0 M	-31	-1 H 34.4 M
		18	-0 H 6.9 M	-32	-1 H 36.7 M
67	4 H 21.0 M	17	-0 H 8.7 M	-33	-1 H 39.1 M
66	3 H 49.7 M	16	-0 H 10.5 M	-34	-1 H 41.6 M
65	3 H 27.9 M	15	-0 H 12.3 M	-35	-1 H 44.1 M
64	3 H 10.7 M	14	-0 H 14.0 M	-36	-1 H 46.7 M
63	2 H 56.2 M	13	-0 H 15.8 M	-37	-1 H 49.3 M
62	2 H 43.8 M	12	-0 H 17.5 M	-38	-1 H 52.0 M
61	2 H 32.8 M	11	-0 H 19.2 M	-39	-1 H 54.9 M
60	2 H 23.0 M	10	-0 H 20.9 M	-40	-1 H 57.8 M
59	2 H 14.2 M	9	-0 H 22.6 M	-41	-2 H .8 M
58	2 H 6.1 M	8	-0 H 24.3 M	-42	-2 H 4.0 M
57	1 H 58.7 M	7	-0 H 25.9 M	-43	-2 H 7.2 M
56	1 H 51.9 M	6	-0 H 27.6 M	-44	-2 H 10.6 M
55	1 H 45.5 M	5	-0 H 29.2 M	-45	-2 H 14.1 M
54	1 H 39.6 M	4	-0 H 30.9 M	-46	-2 H 17.8 M
53	1 H 34.0 M	3	-0 H 32.5 M	-47	-2 H 21.6 M
52	1 H 28.8 M	2	-0 H 34.2 M	-48	-2 H 25.6 M
51	1 H 23.9 M	1	-0 H 35.8 M	-49	-2 H 29.8 M
50	1 H 19.2 M	0	-0 H 37.5 M	-50	-2 H 34.2 M
49	1 H 14.8 M	-1	-0 H 39.1 M	-51	-2 H 38.9 M
48	1 H 10.6 M	-2	-0 H 40.7 M	-52	-2 H 43.8 M
47	1 H 6.6 M	-3	-0 H 42.4 M	-53	-2 H 49.0 M
46	1 H 2.8 M	-4	-0 H 44.0 M	-54	-2 H 54.6 M
45	0 H 59.1 M	-5	-0 H 45.7 M	-55	-3 H .5 M
44	0 H 55.6 M	-6	-0 H 47.3 M	-56	-3 H 6.9 M
43	0 H 52.2 M	-7	-0 H 49.0 M	-57	-3 H 13.7 M
42	0 H 48.9 M	-8	-0 H 50.6 M	-58	-3 H 21.1 M
41	0 H 45.8 M	-9	-0 H 52.3 M	-59	-3 H 29.2 M
40	0 H 42.8 M	-10	-0 H 54.0 M	-60	-3 H 38.0 M
39	0 H 39.9 M	-11	-0 H 55.7 M	-61	-3 H 47.8 M
38	0 H 37.0 M	-12	-0 H 57.4 M	-62	-3 H 58.8 M
37	0 H 34.3 M	-13	-0 H 59.1 M	-63	-4 H 11.2 M
36	0 H 31.6 M	-14	-1 H .9 M	-64	-4 H 25.7 M
35	0 H 29.1 M	-15	-1 H 2.6 M	-65	-4 H 42.9 M
34	0 H 26.5 M	-16	-1 H 4.4 M	-66	-5 H 4.7 M
33	0 H 24.1 M	-17	-1 H 6.2 M	-67	-5 H 36.0 M
32	0 H 21.7 M	-18	-1 H 8.0 M		
31	0 H 19.4 M	-19	-1 H 9.9 M		
30	0 H 17.1 M	-20	-1 H 11.7 M		
29	0 H 14.9 M	-21	-1 H 13.6 M	DECL.	HOUR ANGLE
28	0 H 12.7 M	-22	-1 H 15.5 M		
27	0 H 10.6 M	-23	-1 H 17.5 M		
26	0 H 8.5 M	-24	-1 H 19.5 M		
25	0 H 6.5 M	-25	-1 H 21.5 M		
24	0 H 4.4 M	-26	-1 H 23.5 M		
23	0 H 2.5 M	-27	-1 H 25.6 M		
22	0 H .5 M	-28	-1 H 27.7 M		
21	-0 H 1.3 M	-29	-1 H 29.9 M		
20	-0 H 3.2 M	-30	-1 H 32.1 M		
DECL.	HOUR ANGLE	DECL.	HOUR ANGLE		

TABLE 3

the outputs of three receivers on a single cathode ray tube. Varying noise levels, particularly when man-made interference was present on any one of the receivers, were difficult to compensate for. The preservation of equal signal-to-noise ratios in each of the three outputs was essential in view of the narrow dynamic range of the cathode-ray tube spot intensity and the requirement that a single brilliance setting had to be correct for recording all three signals. This, in fact, is the weakest link in the whole system.

Some samples of the film records are shown in Figure 14. Each sample represents a three-minute interval, but the clocks (and detector current meters) at the side of the film are not shown. Figure 14(a) was recorded at 1830 hours N.Z.S.T. when the diurnal rate is at its lowest, while Figure 14(b) is of a typical high rate period. The three different dot-spacings are quite evident: narrow spacing corresponds to meteors detected on the East antenna, (Receiver - 1), the medium spacing to the North of East antenna (Receiver - 2), and the wide spacing to the South of East antenna (Receiver - 3). In both samples it will be noticed that the lower dot of each medium spaced pair is fainter than the upper dot: this temporary fault was due to a slight inaccuracy in the gain setting of the undelayed signal

through that channel. Such a simple maladjustment can easily happen and its effect is exaggerated by the narrow dynamic range of the cathode-ray tube screen.

In Figure 14(a) there is a total of nine echoes, corresponding to an echo rate of 180 per hour. In Figure 14(b) there are 67 discernable echoes, corresponding to a rate of 1340 per hour. It may be remarked that even if the lowest rate of 180 per hour continued throughout the day the resultant total of over 4000 echoes would be far too many to be handled by the original Clegg method of analysis.

Figure 14(b) shows many echoes which have been detected by more than one antenna, usually by the main beam of one and a side lobe of another. Such cases are easily sorted out by heeding the strongest echo. However, there are four of the 67 echoes which are completely ambiguous and must be disregarded.

A very useful check on the performance of the narrow beam antennas and their associated receivers was provided by a pen recorder which continuously monitored the detector current in each receiver. All records exhibited a prominent peak which recurred every day at the sidereal time corresponding to the passage of the Sagittarius region of the Local Galaxy through the associated antenna beam. This is apparent in Figure 15

which shows superimposed tracings of the records obtained over a period of one fortnight. The differences in beam-width of the antenna arrays are also clearly revealed.

One of the first occasions when the complete triple-antenna system was operating successfully was during July, 1962. The partial rate curves obtained on July 25 are shown in Figure 16. In each of the nine curves the δ-Aquarid shower has produced a very prominent peak, allowing quite a good value to be obtained for its radiant position, as follows:

Right ascension	$337.8^{\circ} \pm 0.5^{\circ}$
Declination	$-13.7^{\circ} \pm 2.9^{\circ}$

These coordinates may be compared with those given by McIntosh (1934), R.A.: 337.7°, Decl.: -18.1° for July 25; and Hoffmeister (1948) who gives R.A.: 333.0°, Decl.: -13.0° for July 26.

The peak in the partial rate curve for the 250-350 Km range interval from the North of East antenna was incomplete because of a gap in the record due to a bad burst of man-made interference. Otherwise the peaks were quite clear and there is no doubt as to their identification. None of the other peaks in these partial rate curves are as prominent, except, perhaps,

for the activity from the East antenna near 0800 hours. However there is very little supporting activity from either of the other two antennas and no radiant can be determined for it. This situation has proved to be surprisingly common, lending support to other evidence (Kaiser, 1961) that meteor showers lose their identity and merge into the sporadic background when large numbers of very faint meteors are being detected.

The above situation is well illustrated by the records obtained in early December, 1962, a time of the year when several well-known southern showers are active (Ellyett, Keay, Roth and Bennett, 1961).

The principal two are the Velids and the Puppids, which, together with the Librids and the Orionids, are marked on the principal rate curves obtained during December 4 (Figure 17) and December 5 (Figure 18). Of the 72 times when a peak should have been present fewer than 5 coincidences were obtained. Even when allowance is made for inaccuracies in the quoted radiant positions there are no clear sequences of peaks (such as that for the δ-Aquarids in Figure 16) which betray shower activity. Furthermore, when the corresponding partial rate curves for each of the two days are intercompared there is very little continuity between them, despite the fact that each of the showers mentioned above lasts

for several days. It is also noticeable that some of the sharper and more prominent peaks one day are replaced by dips in the curve on the next day.

Only the gross characteristics of the partial rate curves relate to one another or persist from day to day: They are the gradual rise in rate from midnight to approximately 0600 hours, the hollow centred near 0900 hours and the broad hump at around 1200-1300 hours followed by the decline in rate towards the evening. Such a finding is consistent with the pattern which emerged from a year-long survey of meteor activity in 1960-61: the broad helion and anti-helion peaks or groupings then also over-shadowed almost all shower activity (Ellyett and Keay, 1963).

7. ACKNOWLEDGEMENT

The work carried out under this grant was greatly facilitated by the provision of test equipment from the Universities of New Zealand Research Grants Committee.

8. REFERENCES

Aspinall, A., Clegg, J.A., and Hawkins, G.S., Phil.Mag., 42, 504, 1951.

Clegg, J.A., Phil.Mag., 34, 577, 1948 a.

Clegg, J.A., J.Brit.Astr.Assoc., 58, 271, 1948 b.

Ellyett, C. and Keay, C.S.L., Mon.Not.R.Astr.Soc., 125, 325, 1963.

Ellyett, C.D., Keay, C.S.L., Roth, K.W., and Bennett,R.G.T., Mon.Not.R.Astr.Soc., 123, 37, 1961.

Ellyett, C.D., and Roth, K.W., Aust.J.Phys., 8, 390, 1955.

Fraser, B.J., M.Sc. Thesis, University of Canterbury, 1961.

Hoffmeister, C., "Meteorstrome" (Weimar), ch.9, 1948.

Kaiser, T.R., Mon.Not.R.Astr.Soc., 123, 265, 1961.

Keay, C.S.L., Aust.J.Phys., 10, 471, 1957.

Keay, C.S.L., and Ellyett, C.D., J.Geophys.Res., 66, 2337, 1961.

Keay, C.S.L., and Gray, R.E., Research Report No.3, Grant NsG-219-62, N.A.S.A., 1963.

McIntosh, R.A., Mon.Not.R.Astr.Soc., 94, 583, 1934.

McLauchlan, E.C., Aust.J.Phys., 13, 750, 1960.

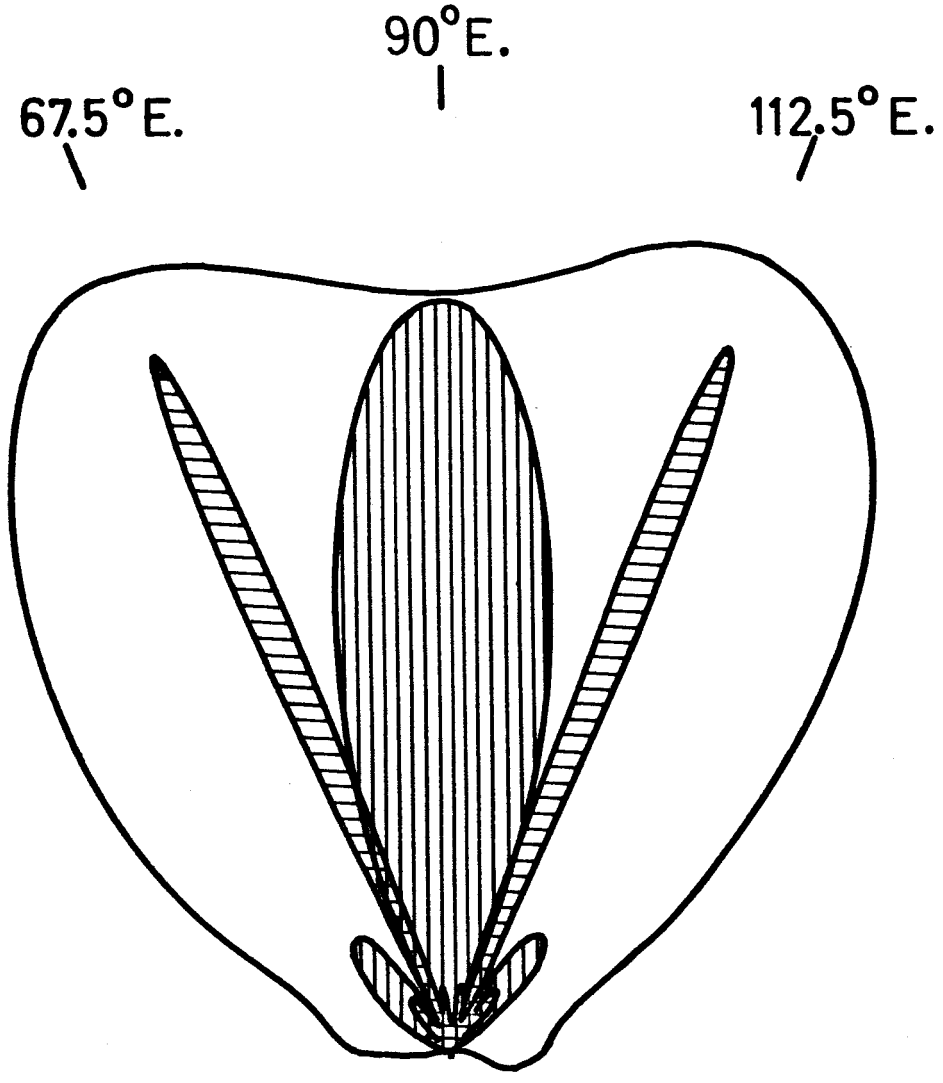

FIGURE 1. Plan view of antenna coverage. The outer curve represents the horizontal radiation pattern of the Fan-Beam transmitting antenna, while the horizontal patterns of the three narrow-beam antennas used for reception are shown shaded.

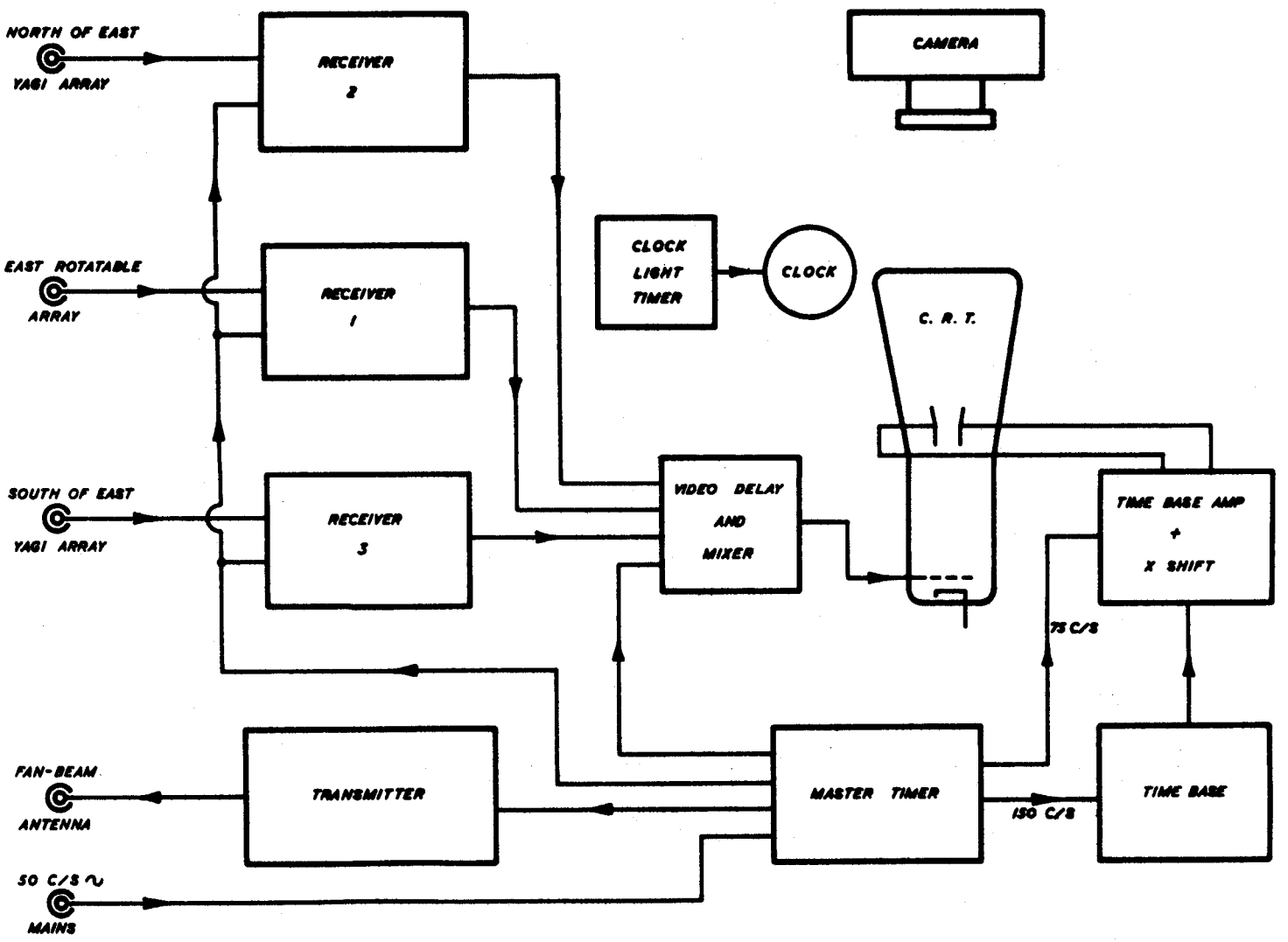

FIGURE 2. BLOCK DIAGRAM OF THE COMPLETE TRIPLE CHANNEL RADAR SYSTEM

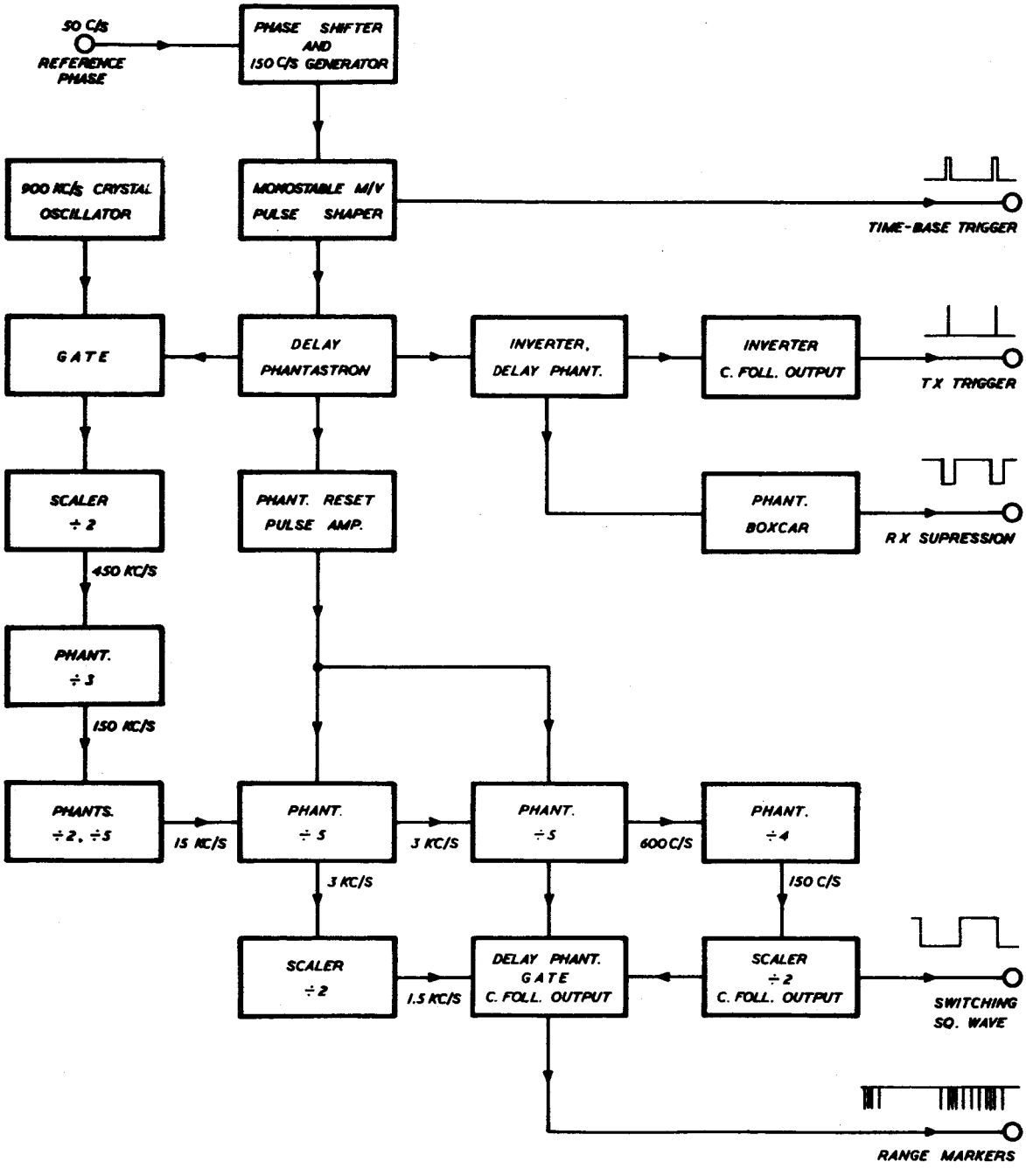

FIGURE 3. BLOCK DIAGRAM OF THE MASTER CONTROL UNIT WHICH SUPPLIES NECESSARY TIMING WAVEFORMS.

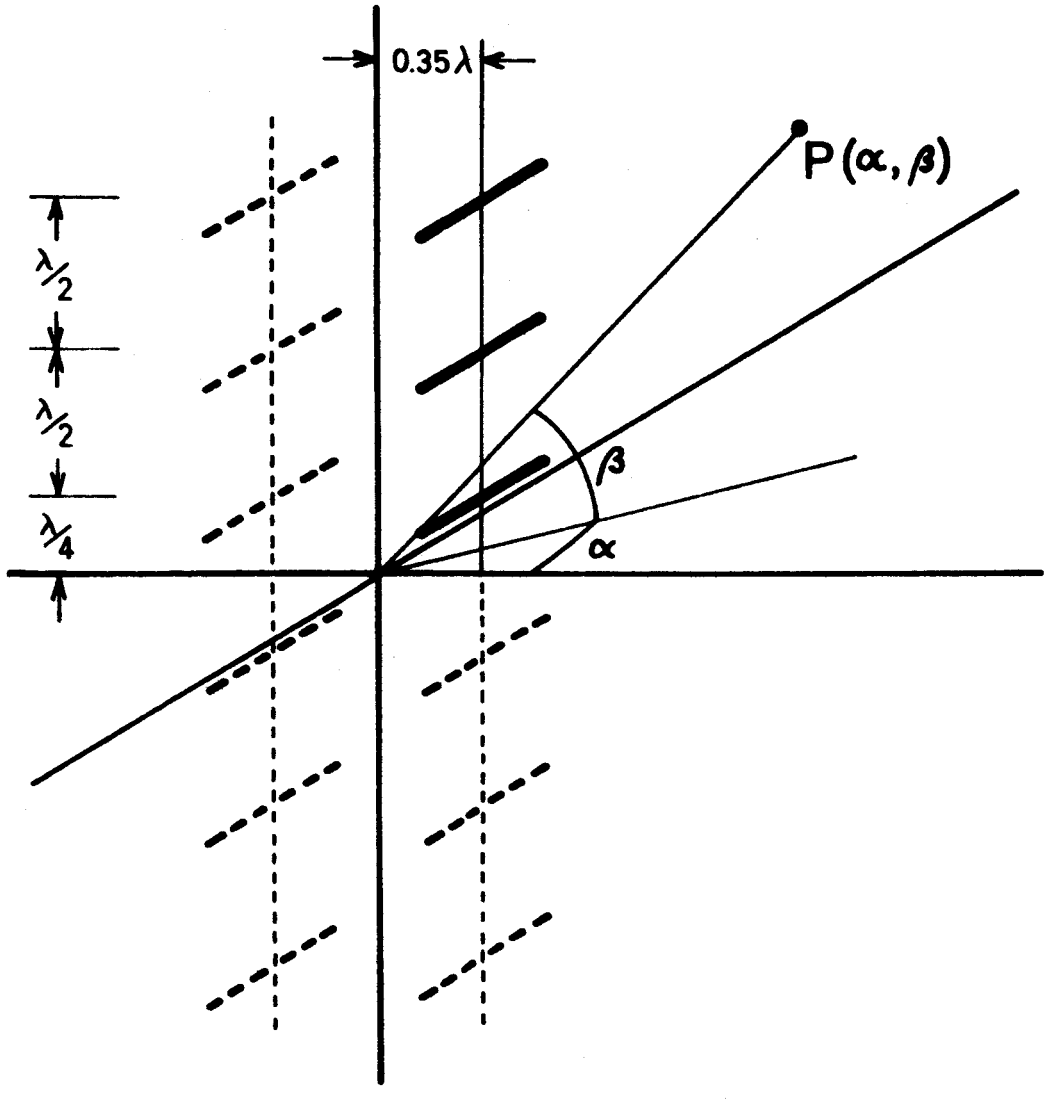

FIGURE 4. GEOMETRY OF THE FAN-BEAM ANTENNA ARRAY, SHOWING IMAGES.

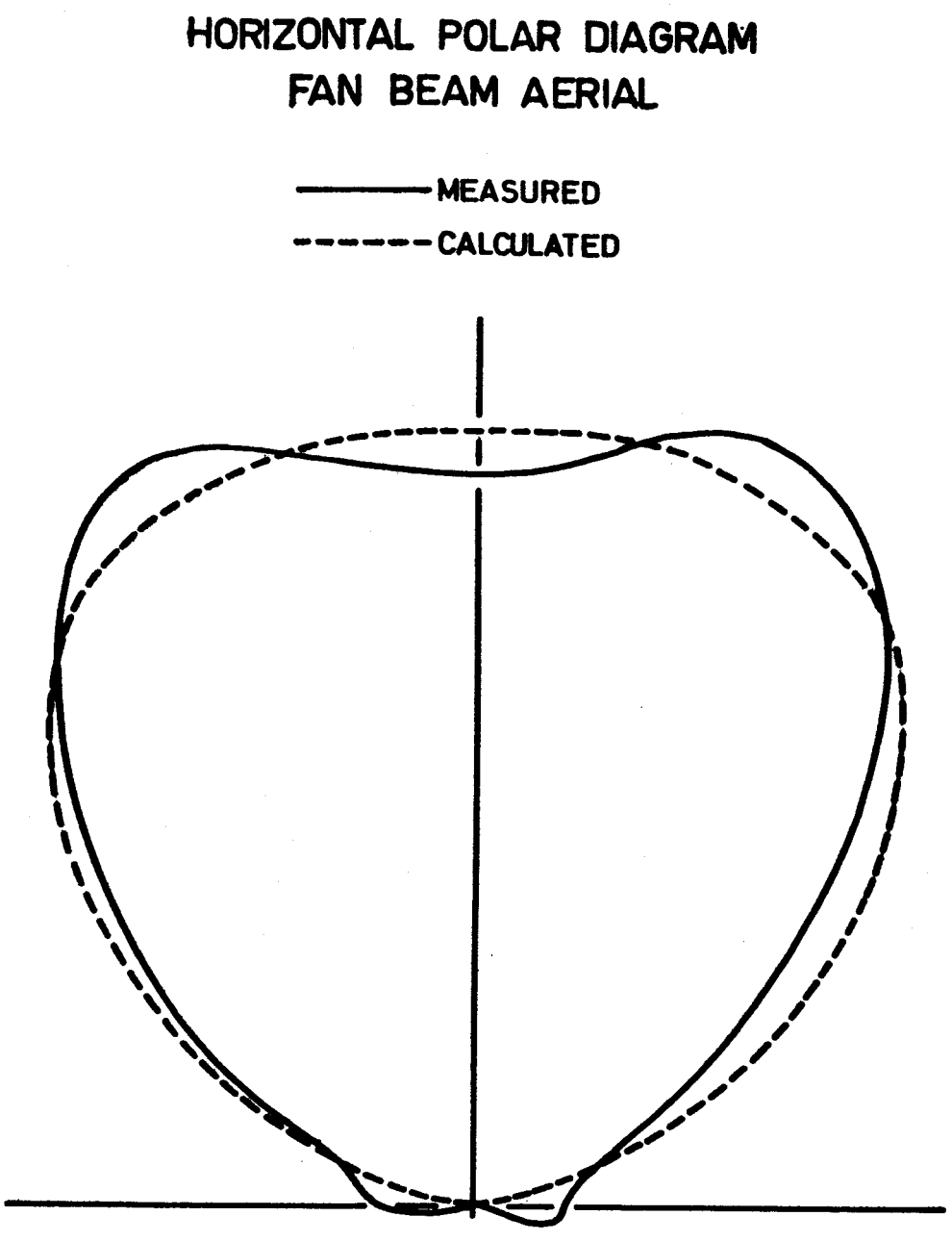

FIGURE 5. Comparison of the measured and calculated horizontal radiation patterns of the Fan-Beam antenna.

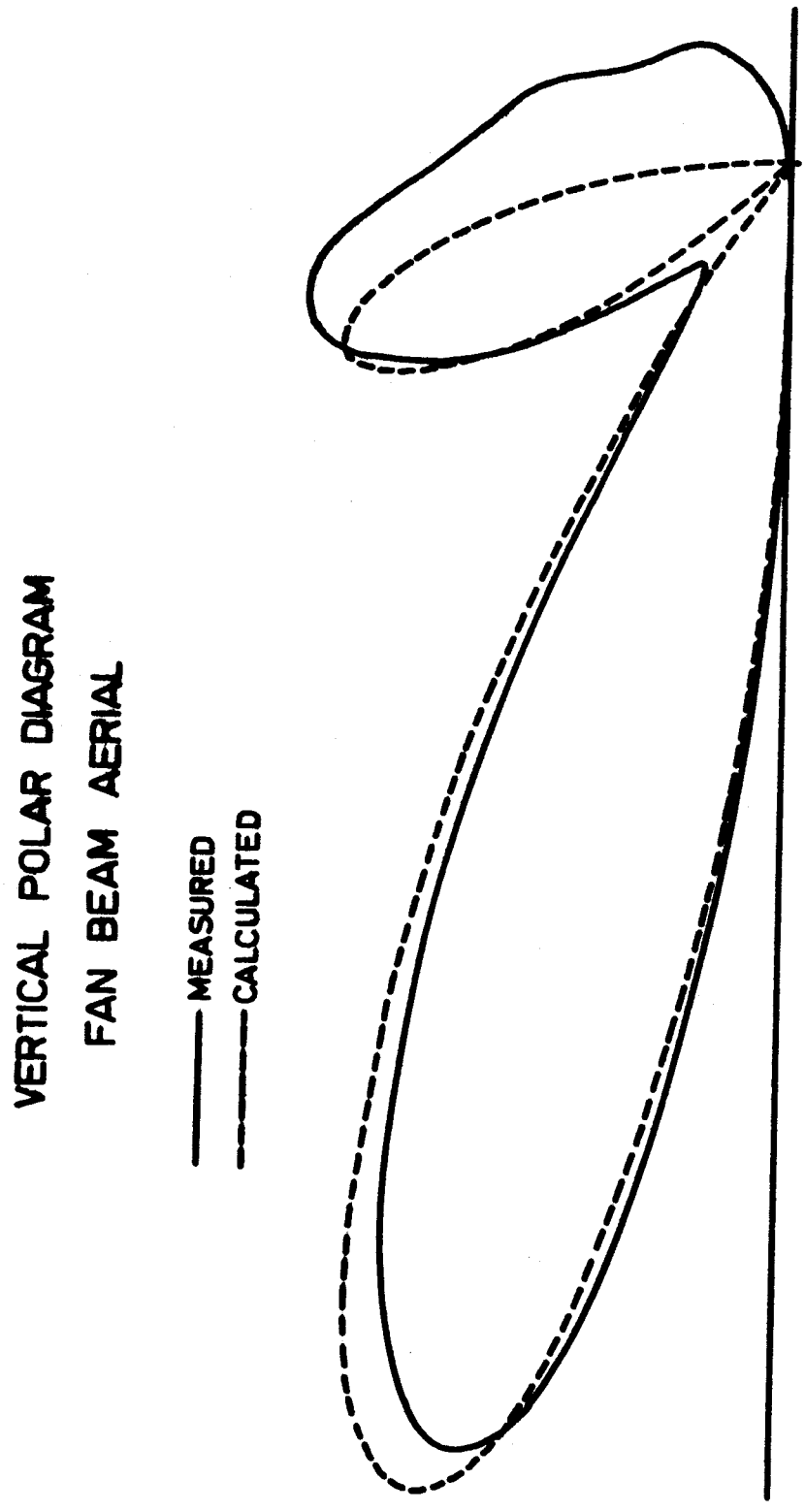

FIGURE 6. Comparison of the measured and calculated vertical radiation patterns of the Fan-Beam antenna.

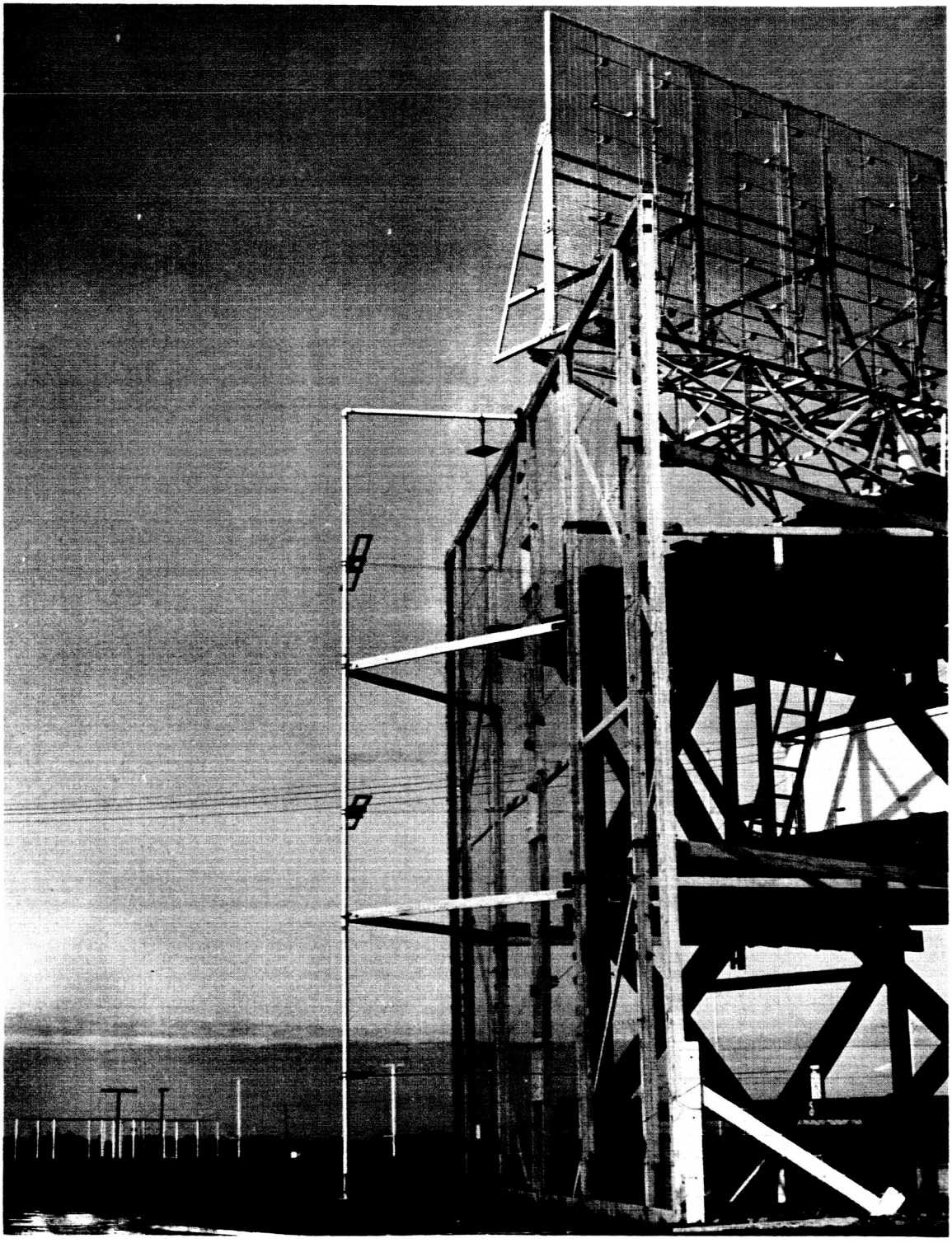

FIGURE 7. THE 69 Mc. FAN-BEAM TRANSMITTING ANTENNA, MOUNTED ON THE SIDE OF AN EXISTING 200 Mc. ROTATABLE ARRAY. A 69 Mc. OMNI-DIRECTIONAL TRANSMITTING ANTENNA IS VISIBLE IN THE BACKGROUND.

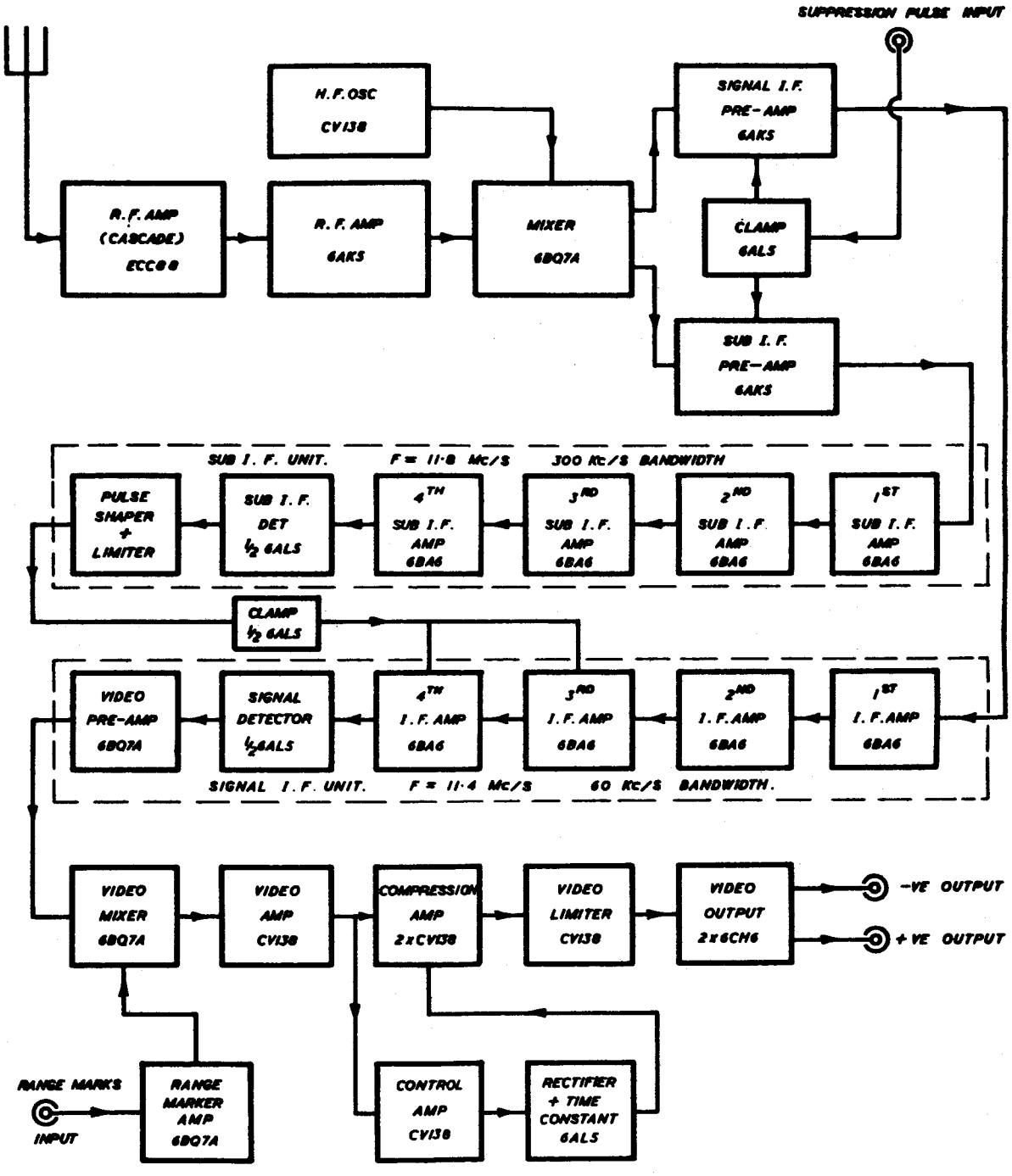

FIGURE 8. RECEIVER BLOCK DIAGRAM

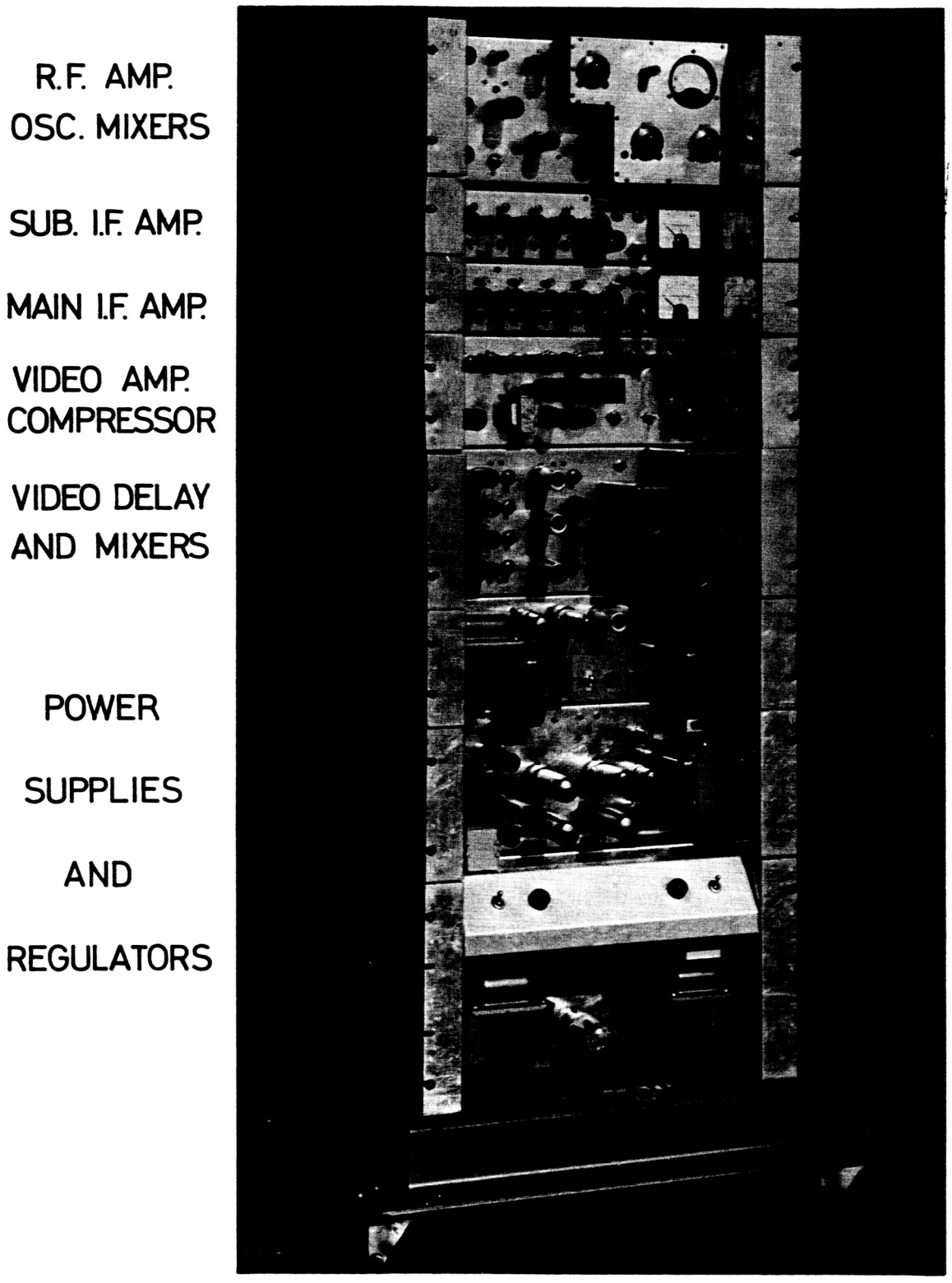

FIGURE 9. ONE OF THE THREE RECEIVERS. THIS RACK ALSO CONTAINS THE VIDEO DELAYS AND MIXING CIRCUITRY.

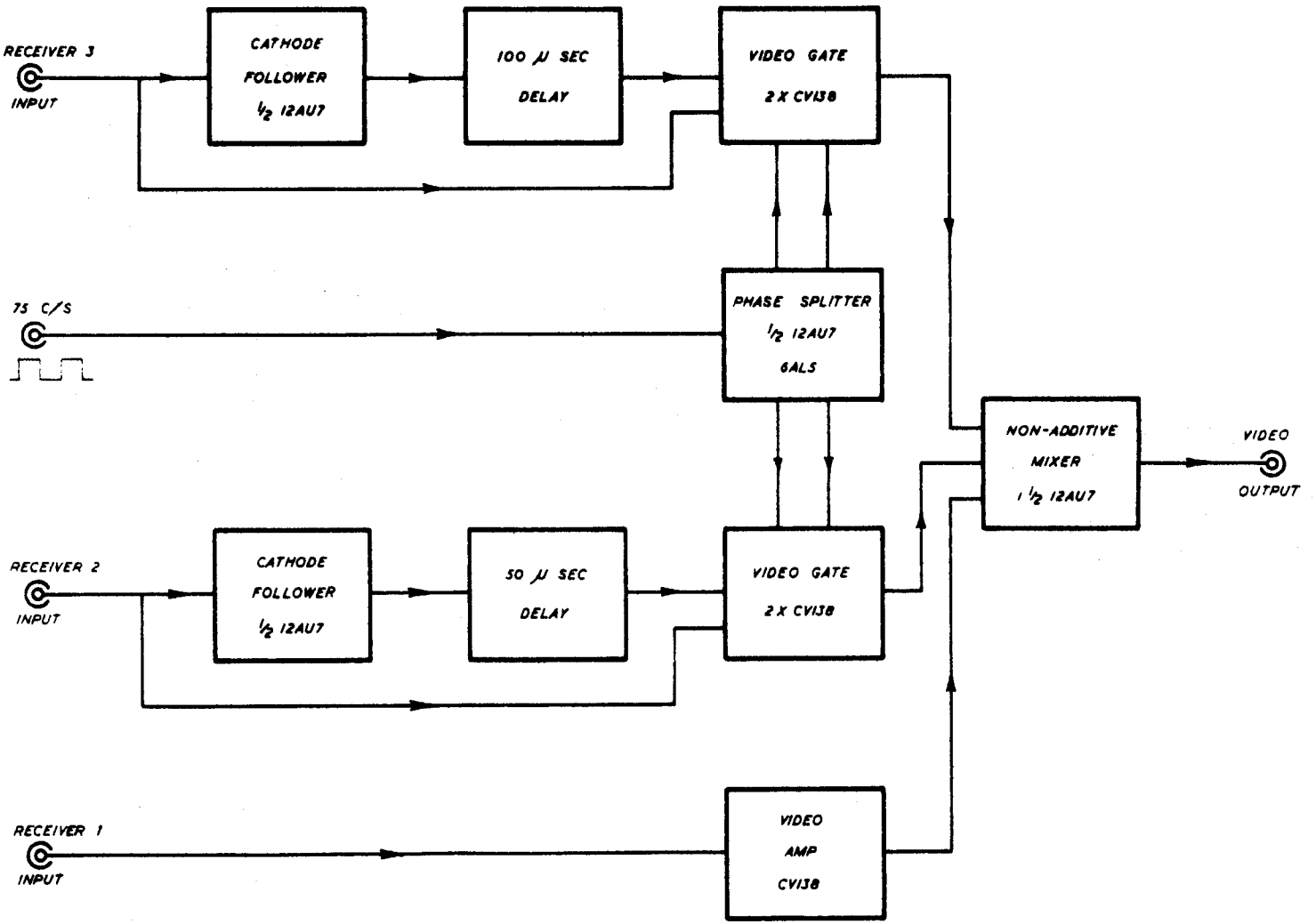

FIGURE 10. BLOCK DIAGRAM OF VIDEO SIGNAL DELAY AND MIXING CIRCUITS.

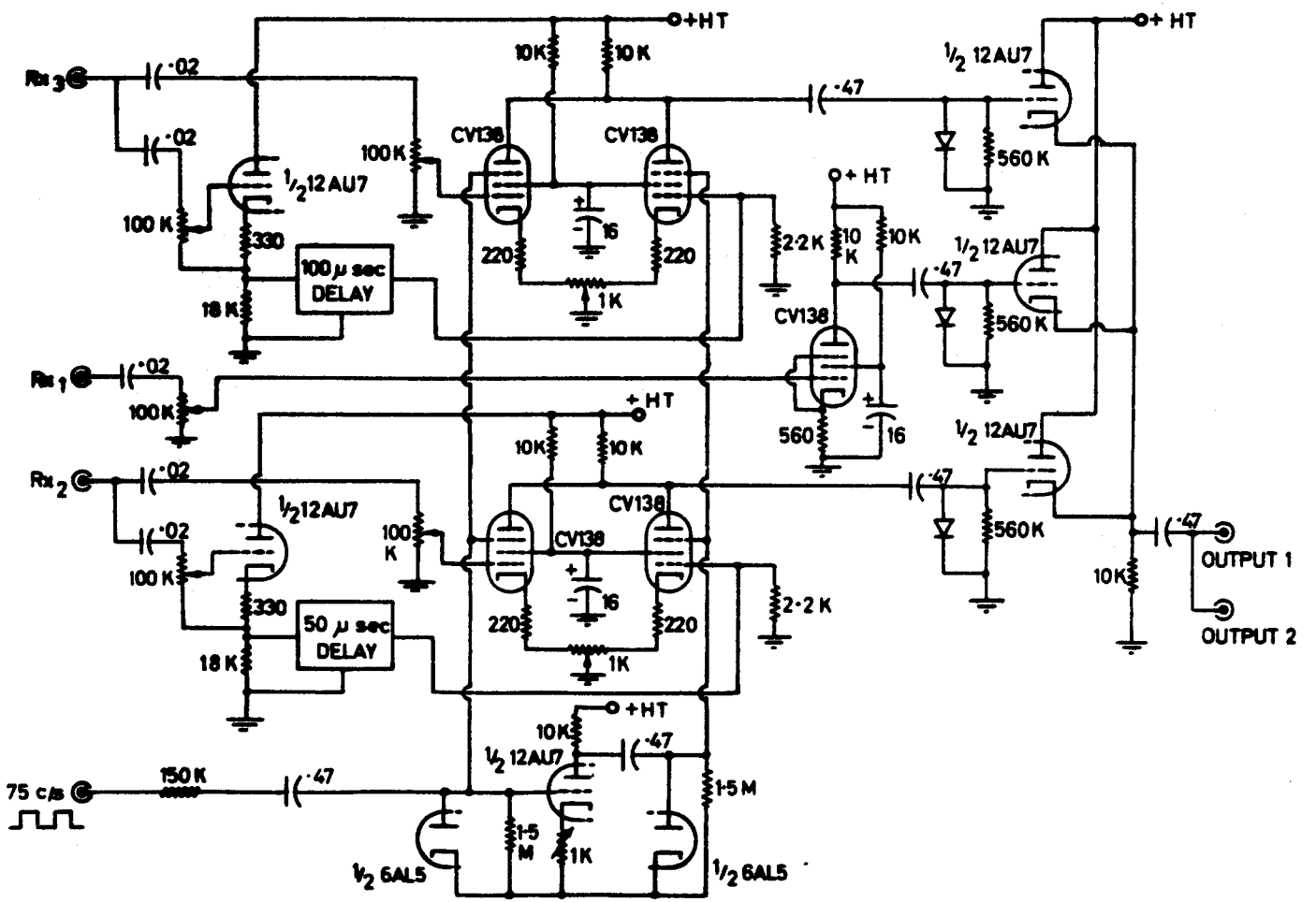

FIGURE 11. VIDEO SIGNAL DELAY AND MIXING CIRCUITS.

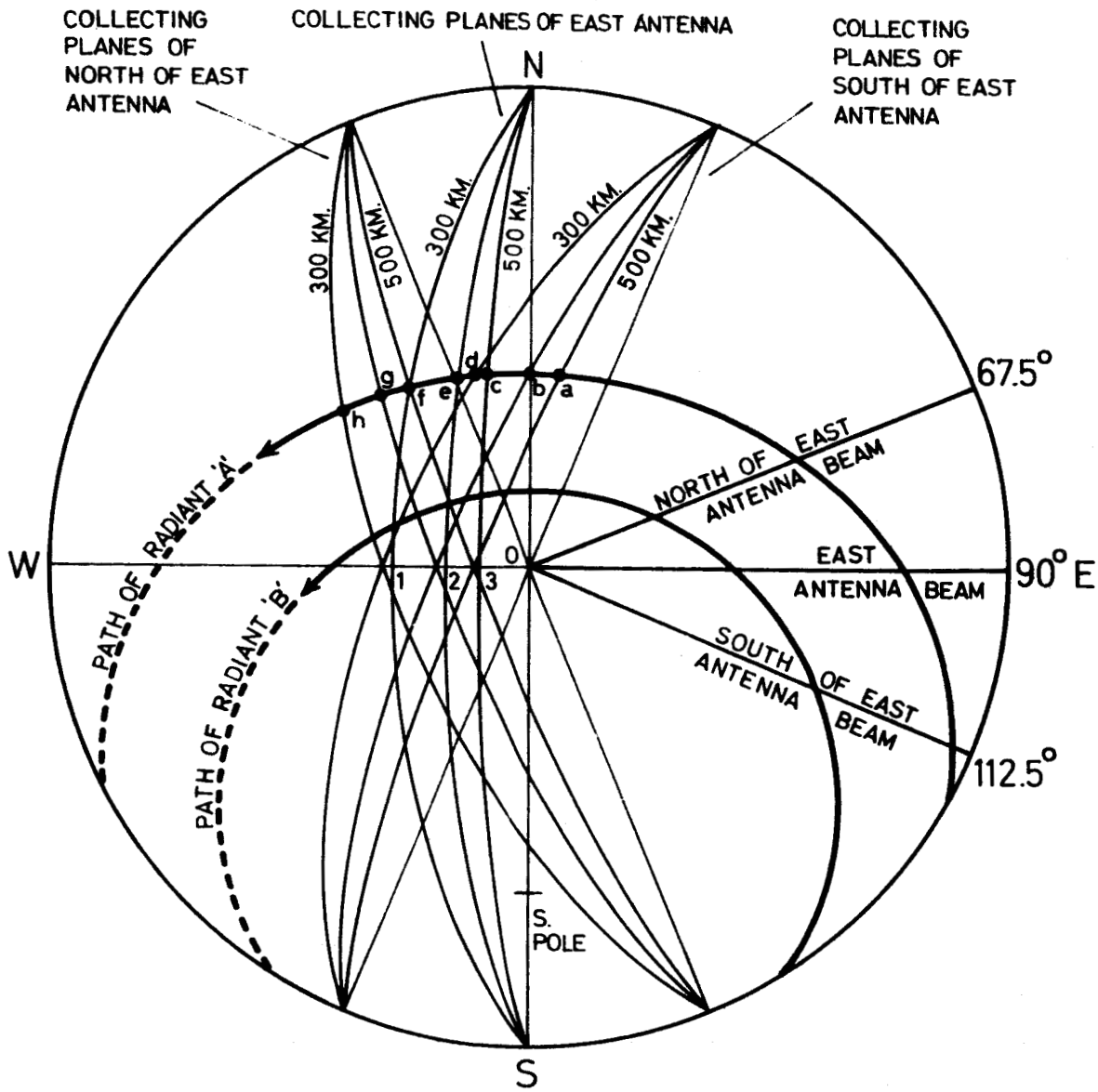

FIGURE 12. HORIZONTAL PROJECTION OF CELESTIAL HEMISPHERE, SHOWING THE COLLECTING PLANES FOR EACH OF THE THREE NARROW BEAM ANTENNAS.

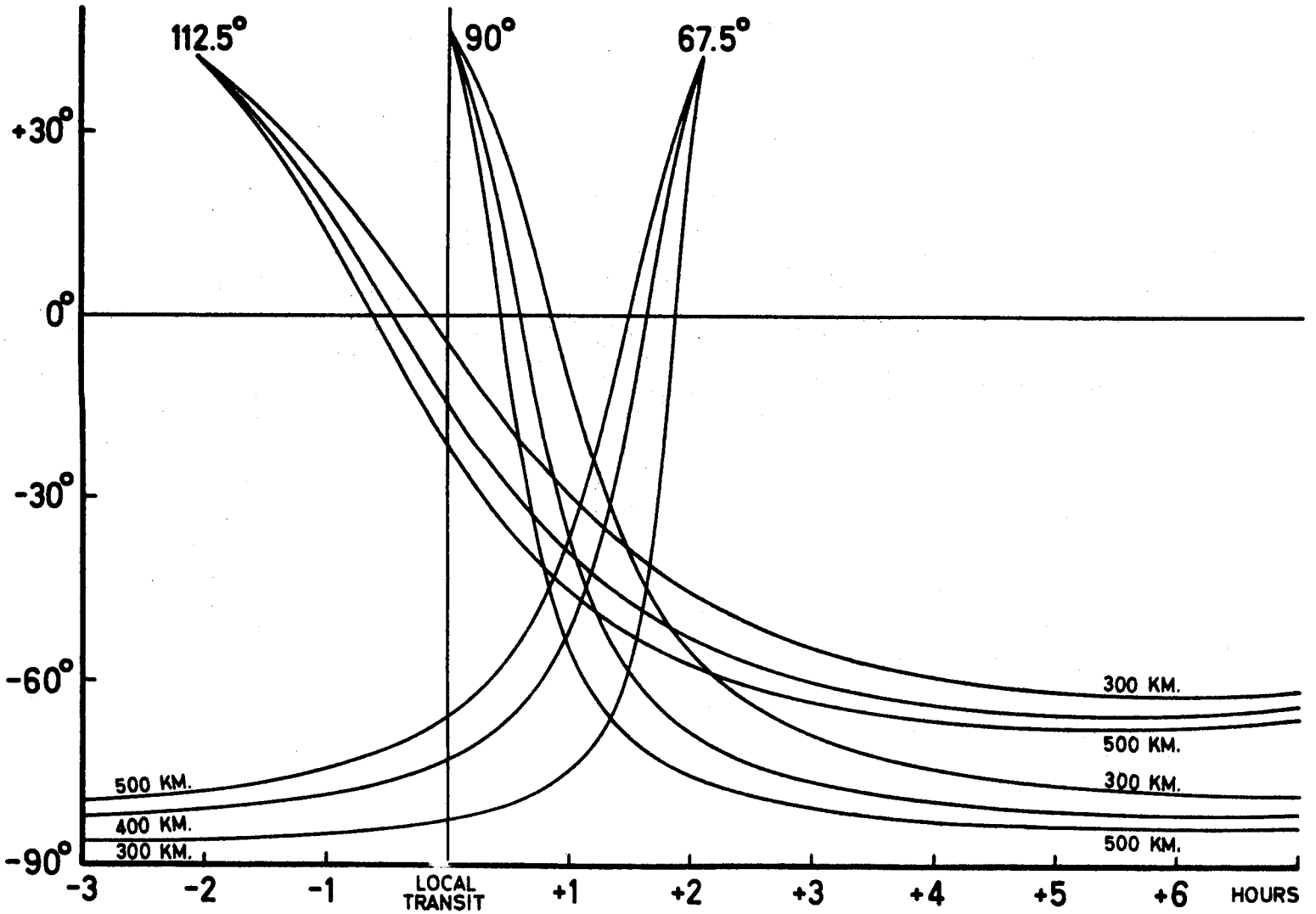

FIGURE 13. TIMES OF RECEPTION OF METEOR ECHOES AT VARIOUS RANGES IN EACH OF THE THREE ANTENNAS, PLOTTED AS A FUNCTION OF RADIANT DECLINATION.

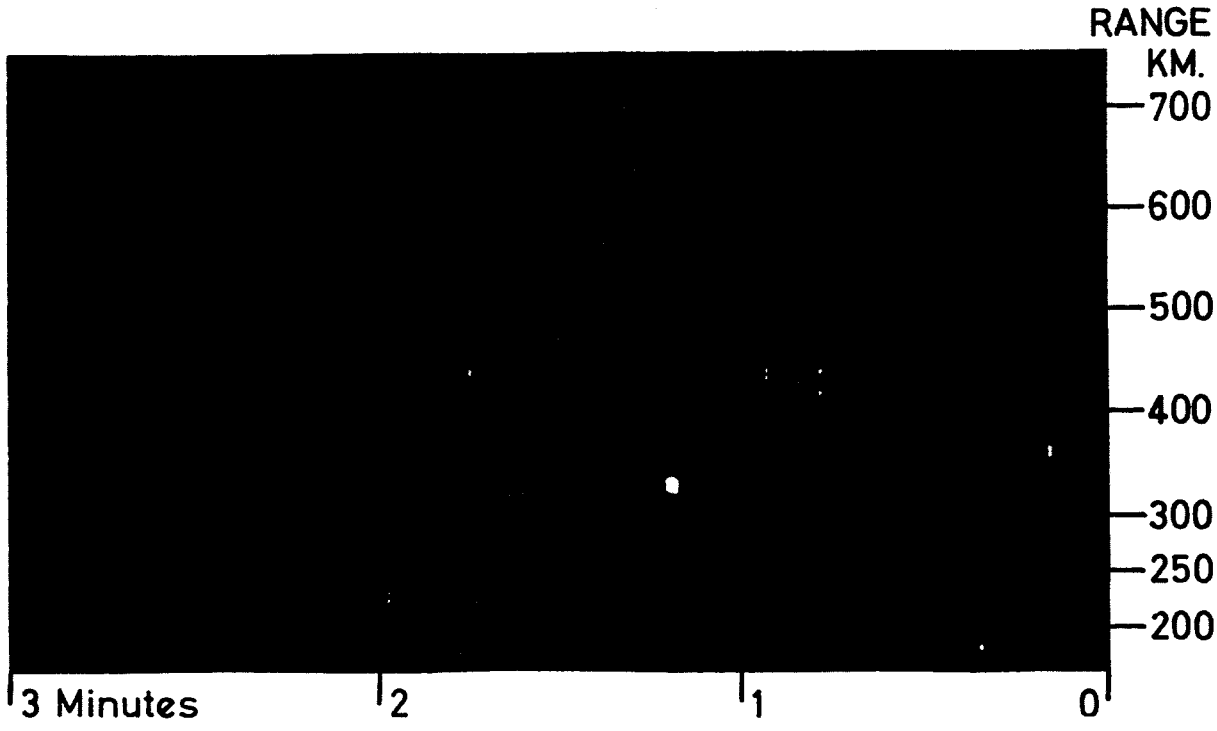

A. 1830 H. N.Z.S.T. 1962 DEC. 9.

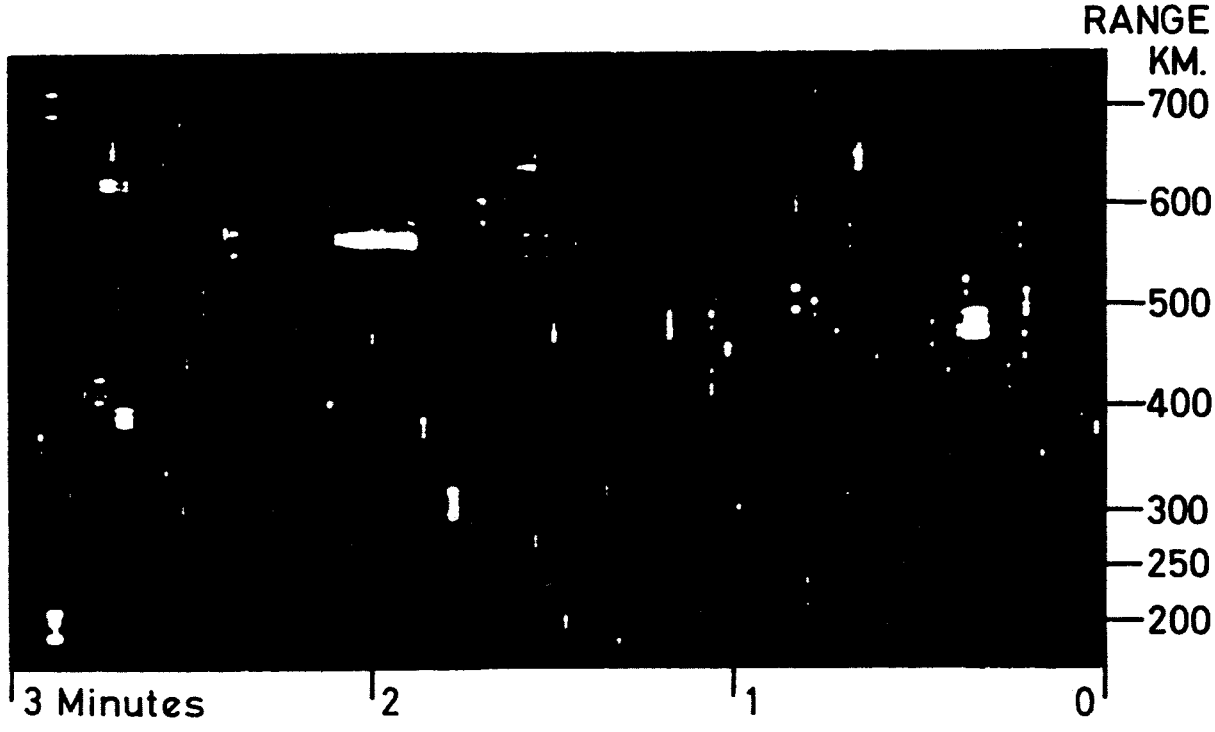

B. 0450 H. N.Z.S.T. 1962 DEC. 5

FIGURE 14. LOW AND HIGH-RATE METEOR ACTIVITY AS SHOWN ON THE FILM RECORDS.

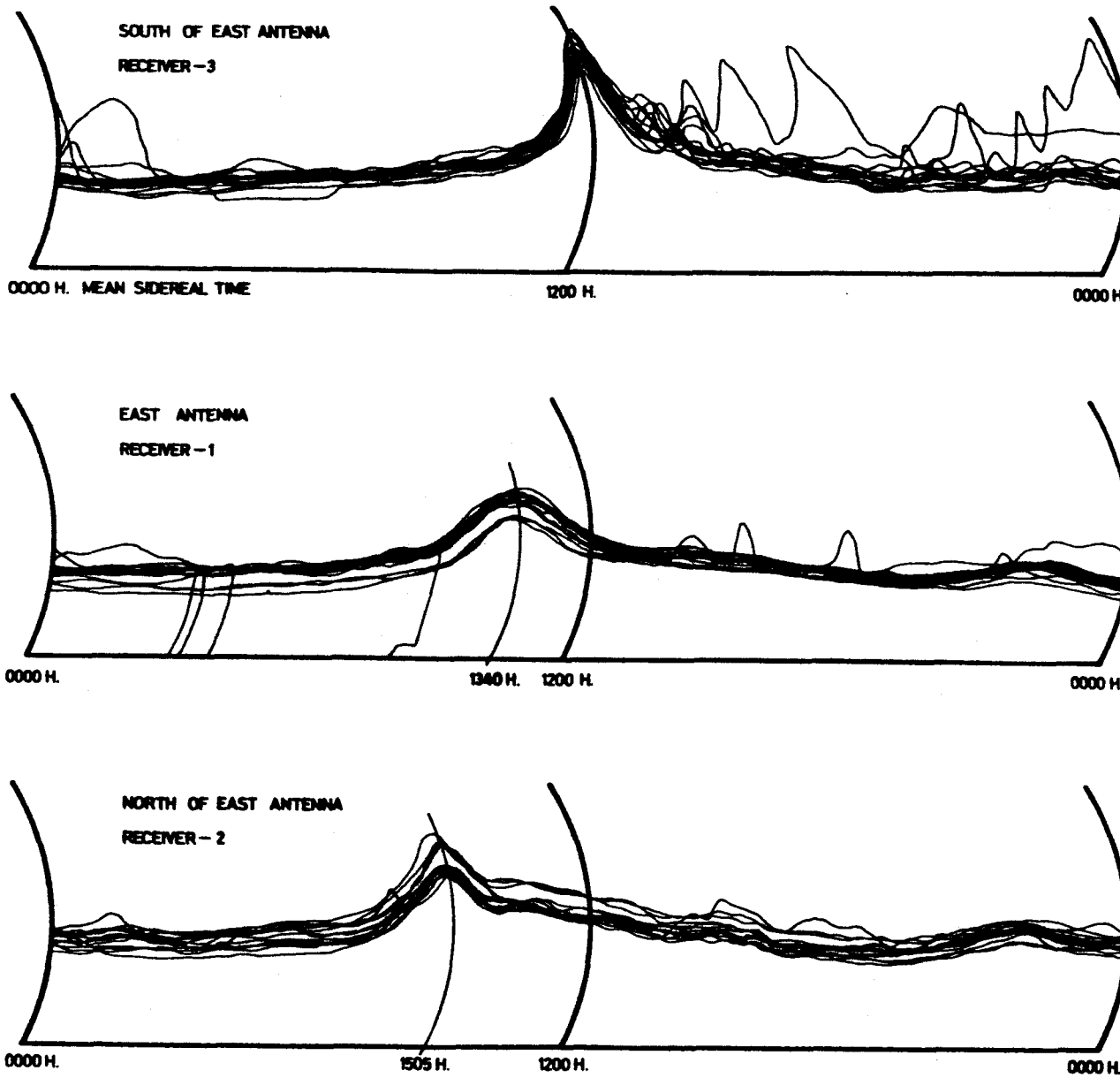

FIGURE 15. Chart tracings of the detector current of each of the three receivers over a period of two weeks (from 23 Nov. to 6 Dec. 1962). In each case the constancy of the receiver sensitivity is revealed by the constant amplitude (relative to the average level) of the noise peak produced by the Sagittarius region of the galaxy as it moves through the respective antenna beam.

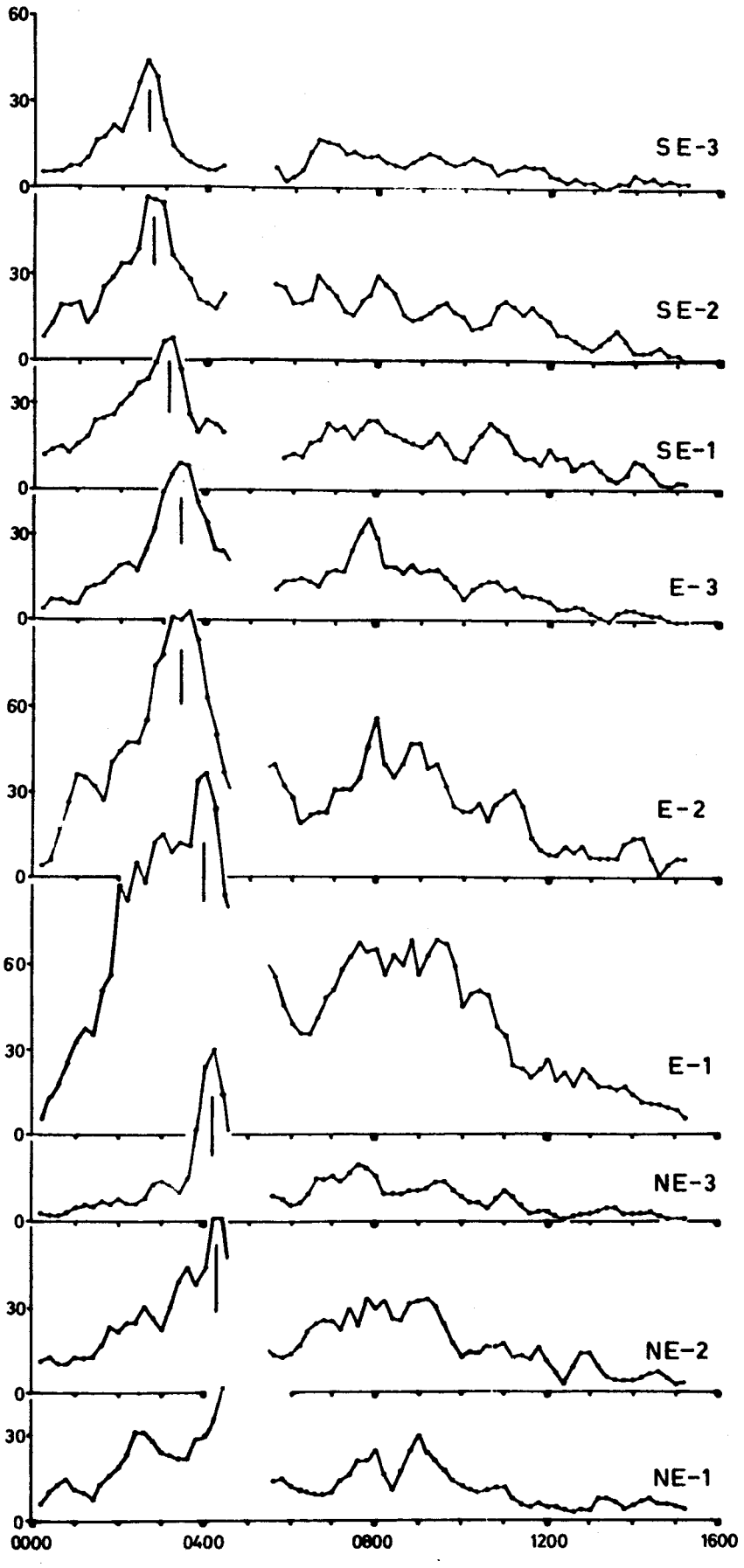

FIGURE 16. PARTIAL RATE CURVES FOR 1962, JULY 25. THE DELTA AQUARID SHOWER IS MARKED.

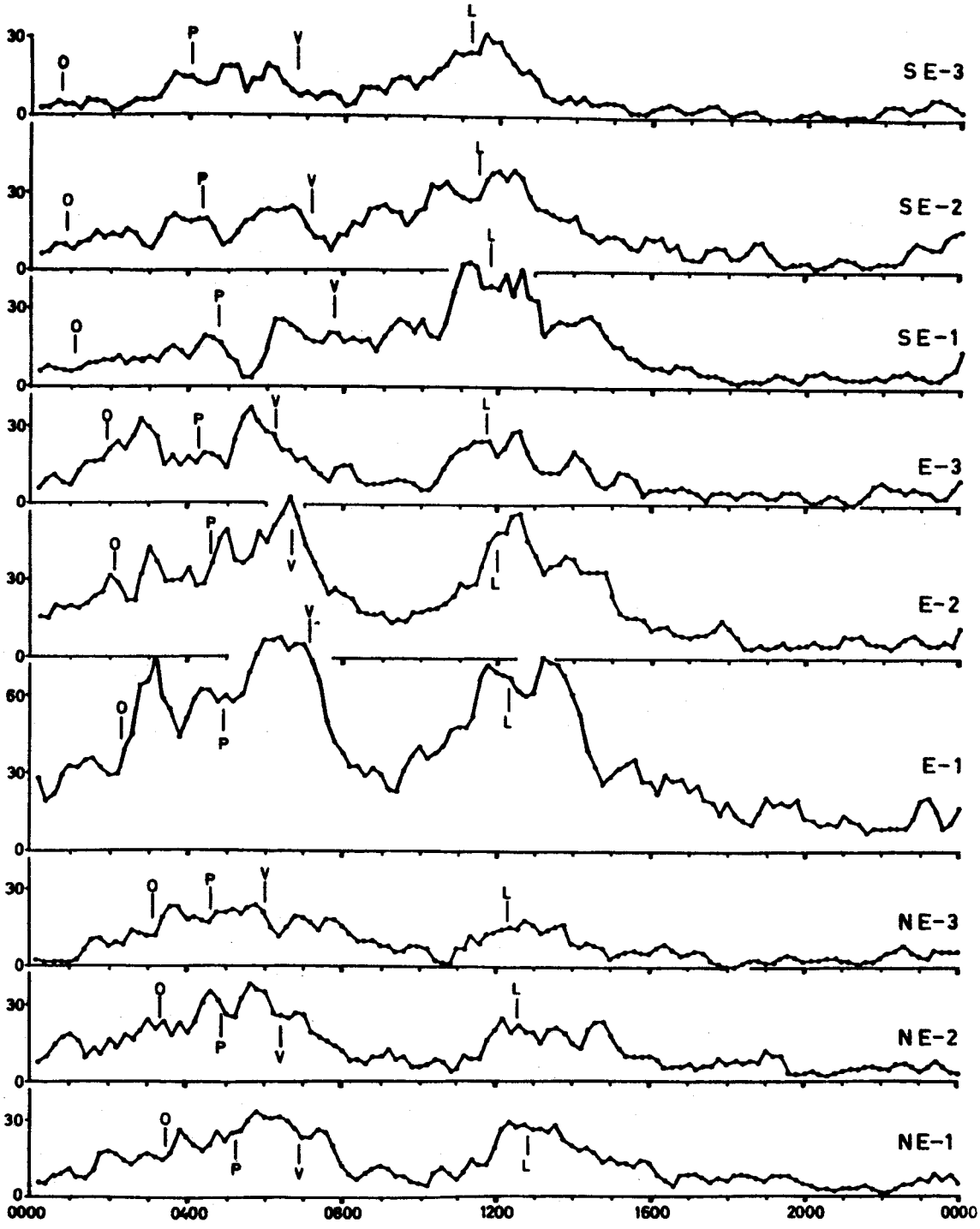

FIGURE 17. PARTIAL RATE CURVES FOR 1962, DECEMBER 4.
"O" IS POSITION OF ORIONID SHOWER (IF PRESENT)
"P" " " " PUPPID " " "
"V" " " " VELID " " "
"L" " " " LIBRID " " "

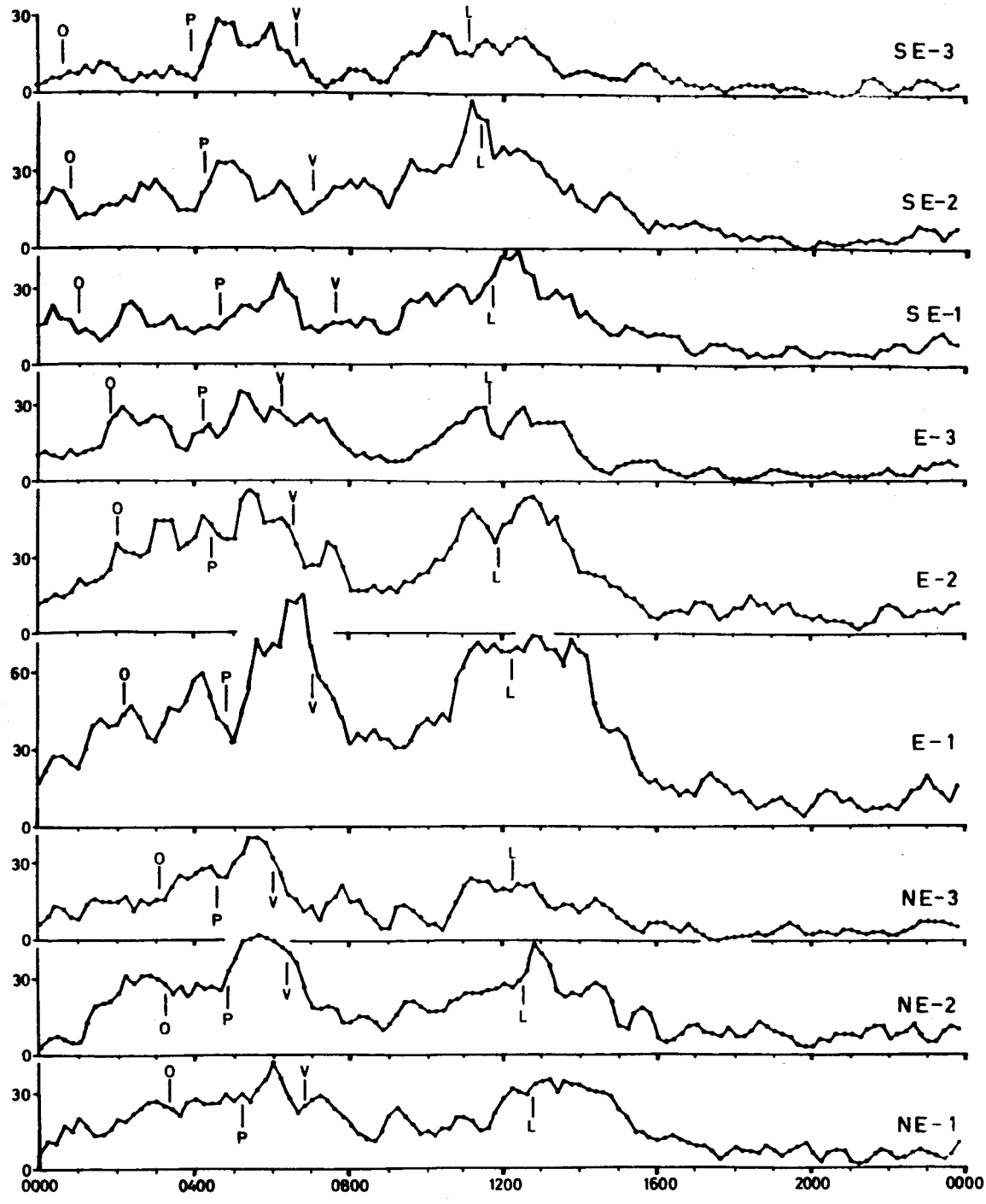

FIGURE 18. PARTIAL RATE CURVES FOR 1962, DECEMBER 5.
"O" IS POSITION OF ORIONID SHOWER (IF PRESENT)
"P" " " " PUPPID " " "
"V" " " " VELID " " "
"L" " " " LIBRID " " "